



Journal Name

ARTICLE

Cysteine redox state plays a key role in the inter-domain movements of HMGB1: A molecular dynamics simulation study

1: A molecular dynamic simulation study

Suresh Panneerselvam, Prasannavenkatesh Durai, Dhanusha Yesudhas, Asma Achek, Hyuk-Kwon Kwon & Sangdun Choi*

Department of Molecular Science and Technology, Ajou University, Suwon 443-749, Korea

***Correspondence**

Sangdun Choi

Department of Molecular Science and Technology, Ajou University, Suwon 443-749, Korea

Fax: +82-31-219-1615

Tel: +82-31-219-2600

E-mail: sangdunchoi@ajou.ac.kr

Table S1. Structural validation of active and inactive states of HMGB1.

S.No.	HMGB1 model	Verify3D	Ramachandran plot (%)		
			Core region	Allowed region	Disallowed region
1	HMGB1 ^{S-S}	86.98%	98.0	2.0	1.9
2	HMGB1 ^{SH-SH}	74.42%	83.3	12.5	4.2
3	HMGB1 ^{SO₃H}	73.95%	83.5	14.2	2.4
4	C23A	74.42%	80.2	16.5	3.3
5	C45A	71.63%	74.5	19.8	5.2
6	C106A	79.07%	81.6	12.7	4.7

Table S2. Active and inactive HMGB1 interaction energies with TLR4/MD2.

Models	Haddock Score	Van der Waals	Electrostatic energy	Desolvation energy	Restraint violent energy	Buried surface area	Z score
HMGB1 ^{SH-SH} (I)	73.3 +/-6.1	-96.8 +/-3.2	-566.5 +/-18.4	92.4 +/-19.6	1378.5+/- 124.63	3411.6+/- 173.1	-2.1
HMGB1 ^{SH-SH} (II)	110.0 +/-48.5	-86.8 +/-8.9	-543.0 +/-8.9	127.6 +/-18.3	1777.7 +/-210.30	3203.7 +/-61.6	-1.5
HMGB1 ^{SH-SH} (III)	80.6 +/-34.1	-95.3 +/-8.2	-301.3 +/-64.0	85.8 +/-13.2	1503.8+/- 145.21	3253.4 +/-99.1	-1.8
HMGB1 ^{SO₃H}	70.7 +/-12.0	-89.0 +/-6.1	-829.3 +/-54.4	151.2 +/-12.1	1743.2+/- 174.46	3643.3+/- 152.4	-2.0
C23A	114.3 +/-10.1	-94.3 +/-8.2	-406.2 +/-338	126.7 +/-6.9	1631.2+/- 160.88	3199.6+/- 252.7	-1.6
C45A	115.6 +/-18.8	-100.6 +/-16.0	-405.6 +/-36.0	92.4 +/-19.6	2049.5 +/-74.58	3018.8+/- 155.0	-1.2
C106A	106.6 +/-22.6	-75.5 +/-8.9	-577.6 +/-100.6	134.5 +/-13.9	1631.2+/- 150.00	2913.5+/- 292.9	-1.5

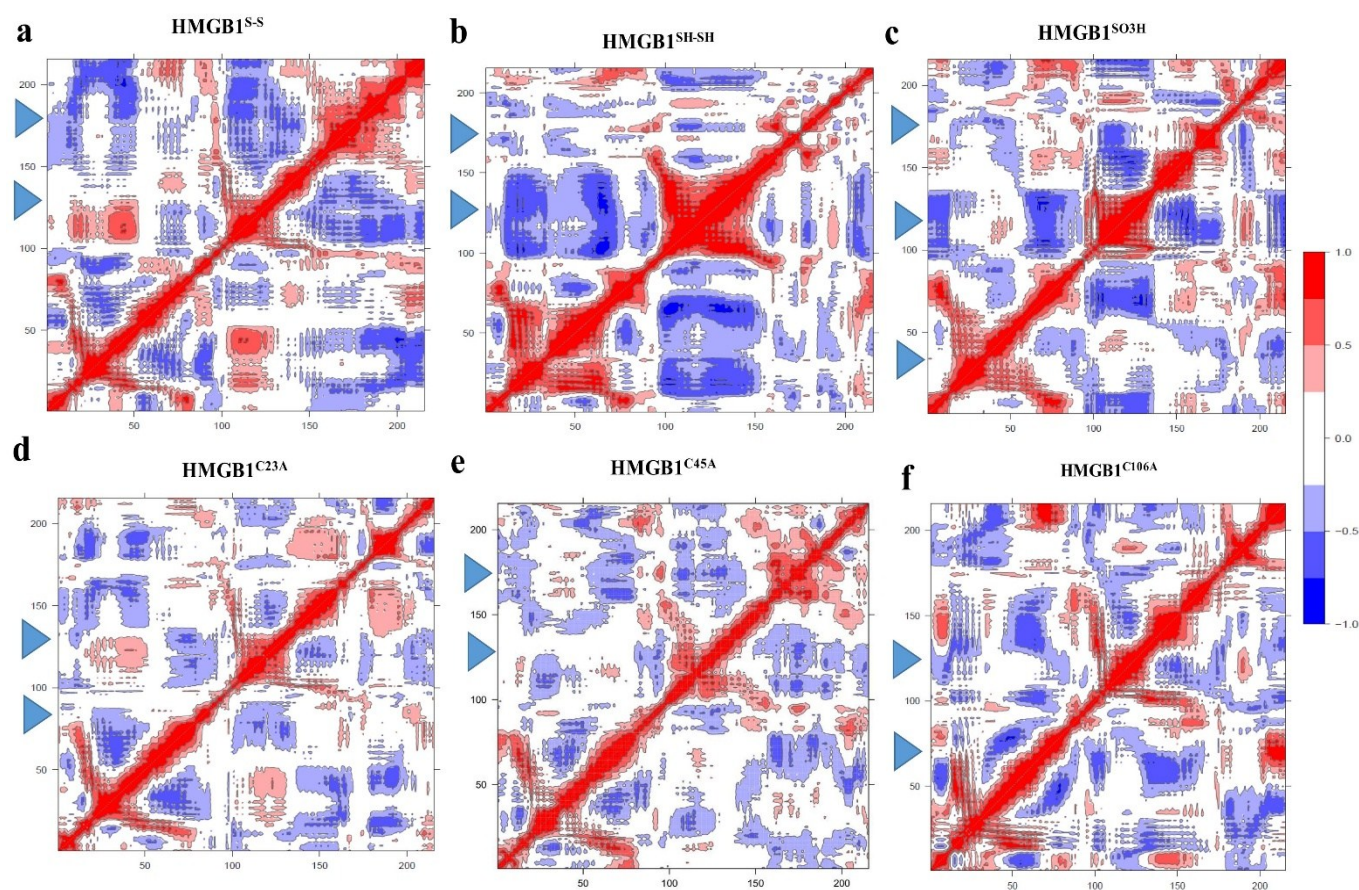


Fig. S1 | Correlation map of HMGB1 isoforms in their redox states. Dynamical cross-correlation maps of (a) HMGB1^{S-S}; (b) HMGB1^{SH-SH}; (c) HMGB1^{SO₃H}; (d) HMGB1^{C23A}; (e) HMGB1^{C45A}; and (f) HMGB1^{C106A}. The color scale indicates the degree of correlation: Red cross-correlations indicate correlated motion (motion in the same direction). Blue cross-correlations indicate anti-correlated motions (motion in the opposite direction). Changes are marked with a blue triangle.

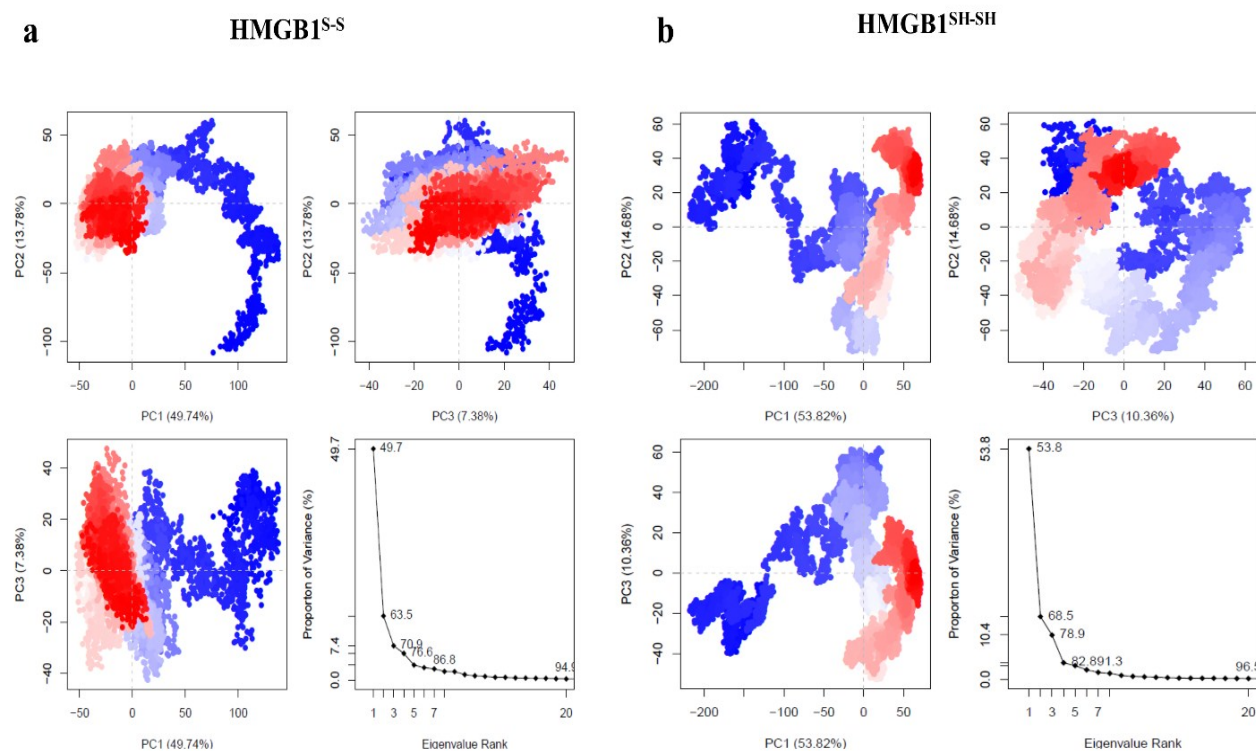


Fig. S2 | Principal Component Analysis (PCA) of HMGB1^{S-S} and HMGB1^{SH-SH}. (a) PCA of HMGB1^{S-S}. Projections of the simulated trajectories of HMGB1^{S-S} on the three principal component (PCs) derived from PCA. Scores for the first, second, and third PCs of HMGB1^{S-S} were 49.74%, 13.78%, and 7.38% respectively. (b) PCA of HMGB1^{SH-SH}. Projections of the simulated trajectories of HMGB1^{SH-SH} on the three PCs derived from PCA. Scores for the first, second, and third PCs for HMGB1^{SH-SH} were 53.82%, 14.68%, and 10.36% respectively. The first three PCs cover 78.9% of the overall motion for HMGB1^{SH-SH}. The color scale tracks the trajectory numbers from blue to red in order of time. The continuous color scale (from blue to white to red) indicates that there are periodic jumps between these conformers throughout the trajectory.

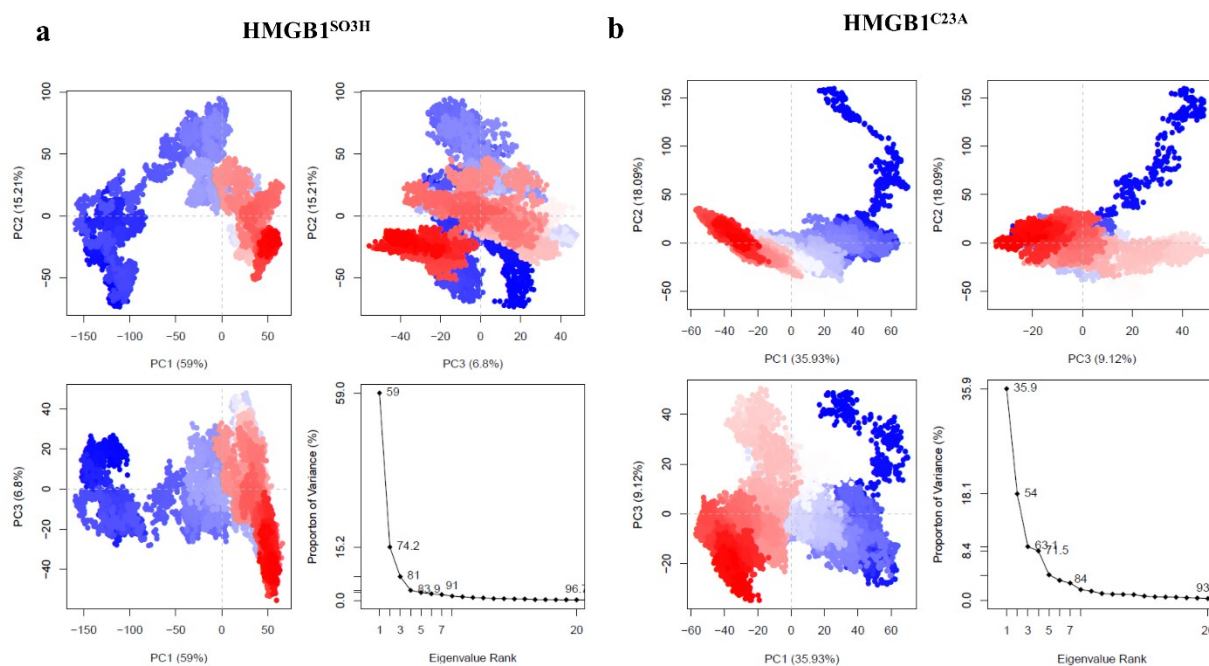


Fig. S3 | Principal Component Analysis (PCA) of HMGB1^{SO3H} and HMGB1^{C23A}. (a) PCA of HMGB1^{SO3H}. Projections of the simulated trajectories of HMGB1^{SO3H} on the three principal components (PCs) derived from PCA. Scores for the first, second, and third PCs for HMGB1^{SO3H} were 59%, 15.21%, and 6.8% respectively. The first three PCs cover 81% of the overall motion for HMGB1^{SO3H}. (b) PCA of HMGB1^{C23A}. Projections of the simulated trajectories of HMGB1^{C23A} on the three PCs derived from PCA. Scores for the first, second, and third PCs for HMGB1^{C23A} were 35.93%, 18.09%, and 9.12% respectively. The first three PCs cover 63% of the overall motion for HMGB1^{C23A}. The color scale tracks the trajectory numbers from blue to red in order of time. The continuous color scale (from blue to white to red) indicates that there are periodic jumps between these conformers throughout the trajectory.

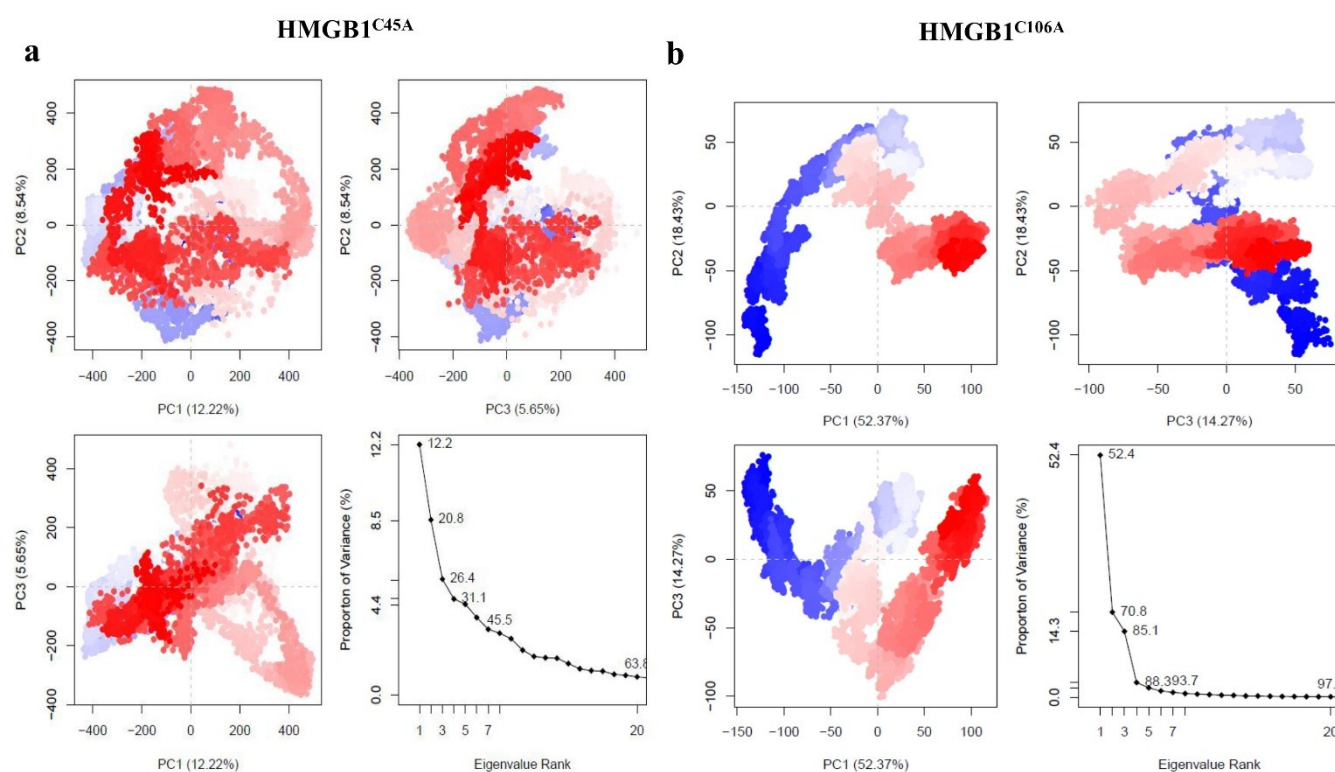


Fig. S4 | Principal Component Analysis (PCA) of HMGB1^{C45A} and HMGB1^{C106A}. (a) PCA of HMGB1^{C45A}. Projections of the simulated trajectories of HMGB1^{C45A} on the three principal components (PCs) derived from PCA. Scores for the first, second, and third PCs for HMGB1^{C45A} were 12.22%, 20.8%, and 26.4% respectively. The first three PCs cover 59.06% of the overall motion for HMGB1^{C45A}. (b) Projections of the simulated trajectories of HMGB1^{C106A} on the three principal components (PCs) derived from PCA. Scores for the first, second, third PCs for HMGB1^{S-S} were 52.37%, 18.43%, and 14.27% respectively. The first three PCs cover 63% of the overall motion for HMGB1^{C106A}. We performed the analysis for the 100 ns trajectory. The color scale tracks the trajectory numbers from blue to red in order of time. The continuous color scale (from blue to white to red) indicates that there are periodic jumps between these conformers throughout the trajectory.

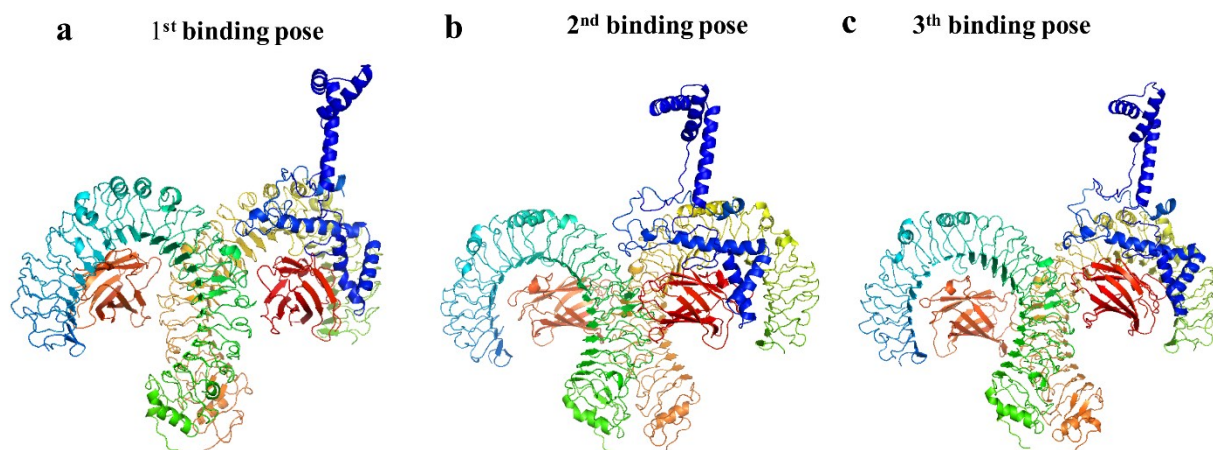


Fig. S5 | Three docked binding poses of TLR4/MD2/HMGB1^{S-S}. The docked HMGB1^{S-S} model is shown in blue. The B-box domain of HMGB1^{S-S} is bound to the TLR4/MD2 complex, and the only changes observed are in the orientation of the A-box domain.

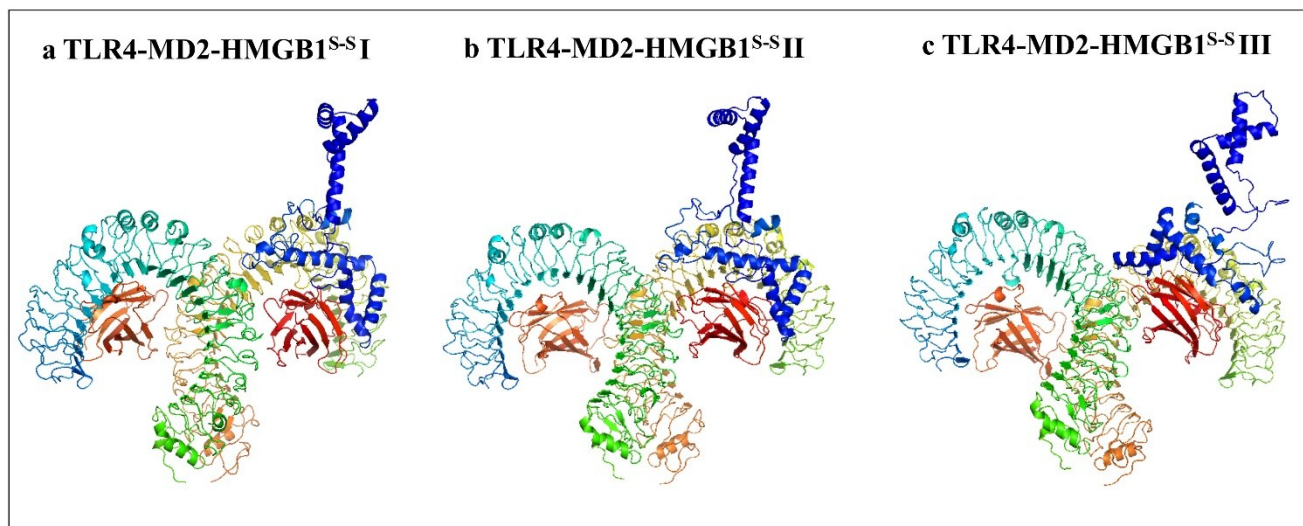


Fig. S6 | HMGB1^{S-S} relevant docked conformations. Three docked conformations of HMGB1^{S-S}. The three HMGB1 structures can also be seen in Fig. 3.

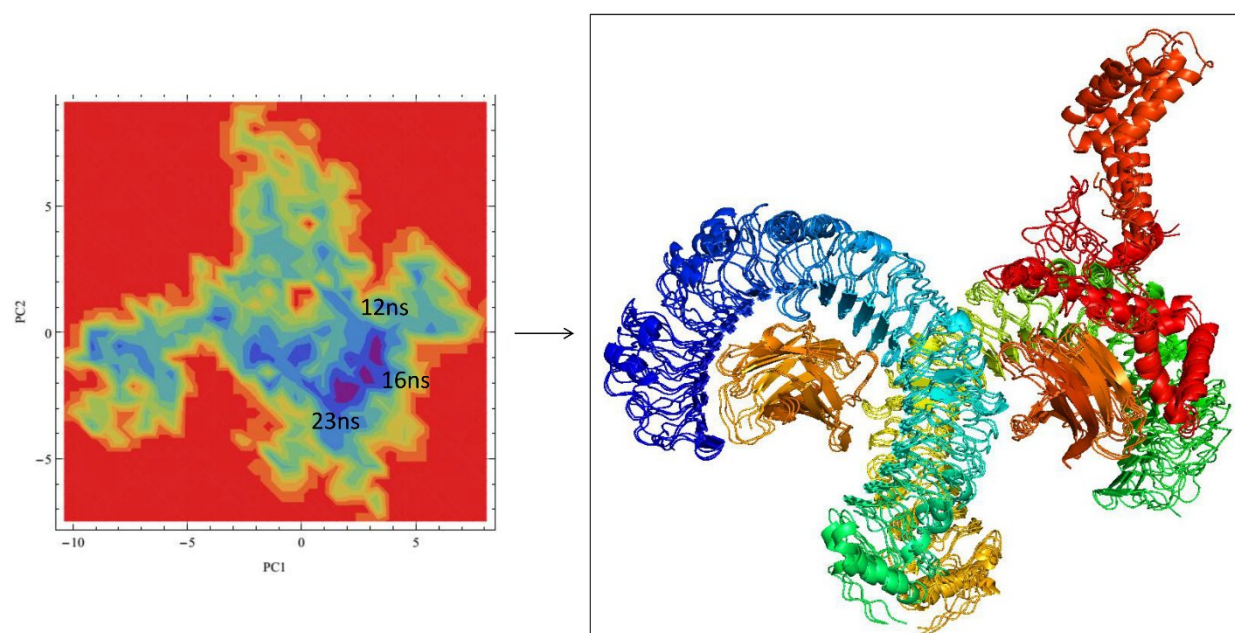


Fig. S7 | Free Energy Landscape (FEL) of simulated model complex of TLR4/MD2/HMGB1^{S-S}. FEL representation calculated using the first two principal components as reaction coordinates. The major basins are labeled (I to III). Representative structures from the three states are shown, including the minor intermediate state (I), the major intermediate state (II), and the folded state (III). On the right, the lowest energy structures of TLR4/MD2/HMGB1^{S-S} are superimposed.

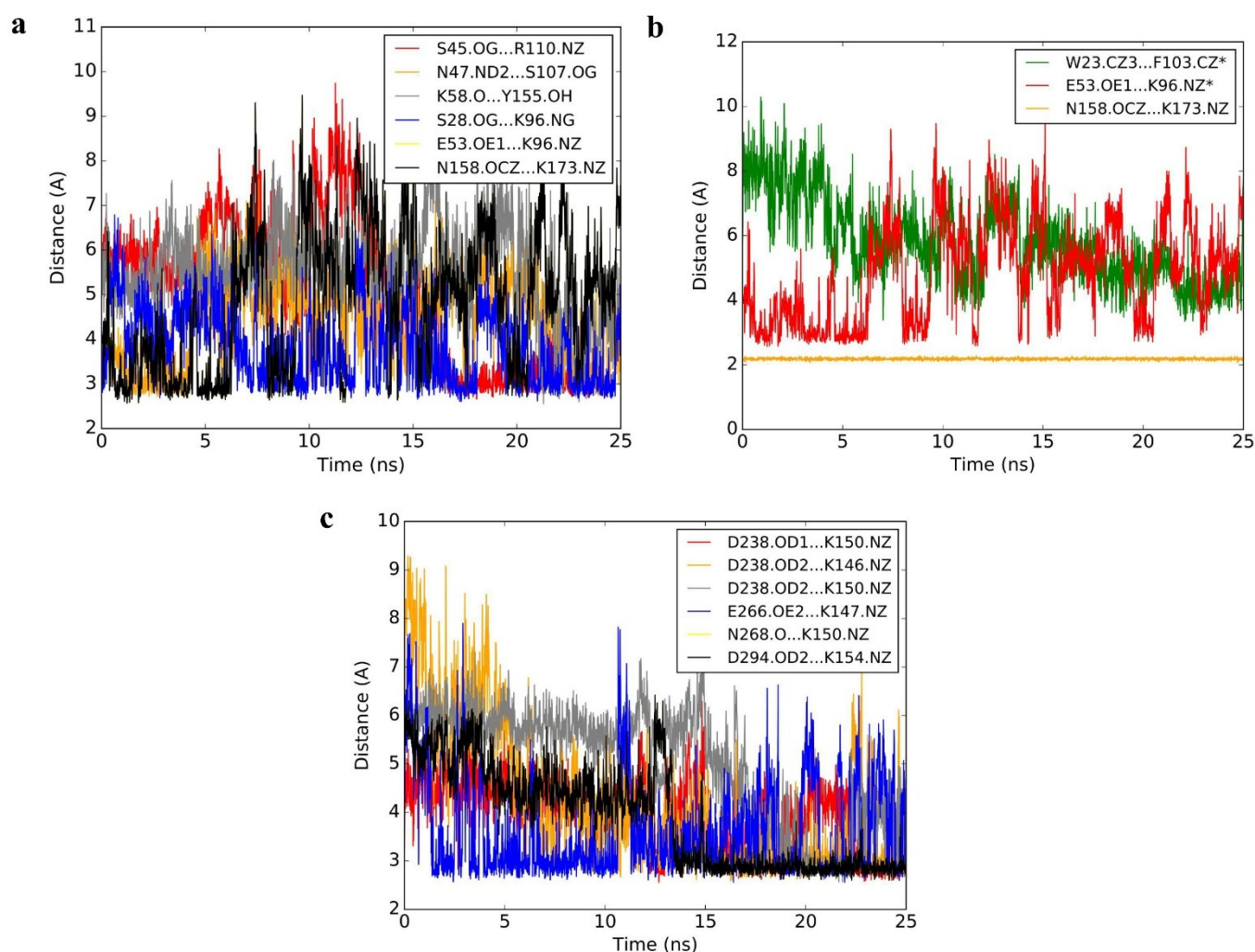


Fig. S8 | Stability of the bonds between TLR4/MD2/HMGB1^{S-S}. (a) Hydrogen bond interactions of MD2 and HMGB1^{S-S}. (b) Hydrophobic and ionic interactions of MD2 and HMGB1^{S-S}. (c) Hydrogen and ionic bond interactions of TLR4 and HMGB1^{S-S}.

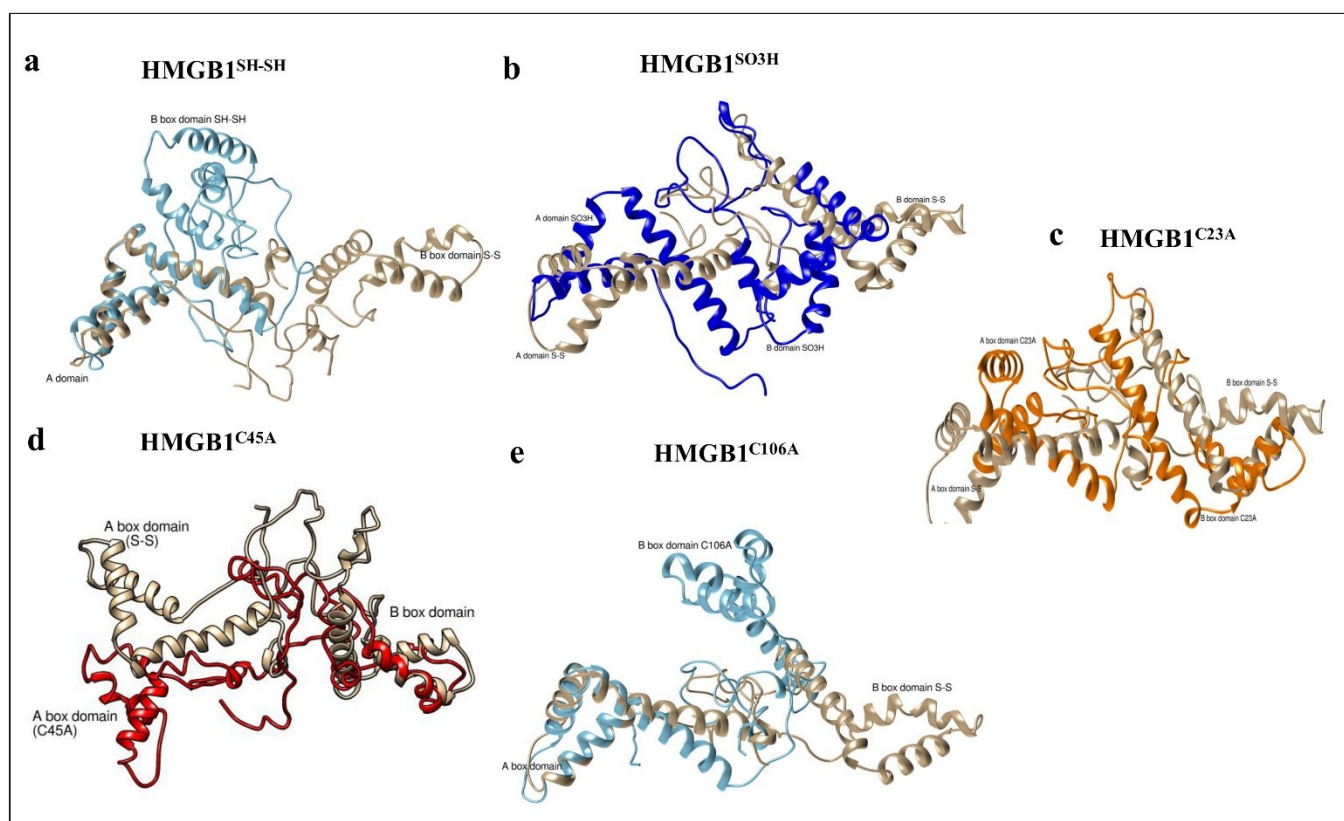


Fig. S9 | Comparison of HMGB1 structures in different redox states. (a) Superimposition of HMGB1^{S-S} and HMGB1^{SH-SH}. (b) Superimposition of HMGB1^{S-S} and HMGB1^{SO3H}. (c) Superimposition of HMGB1^{S-S} and HMGB1^{C23A}. (d) Superimposition of HMGB1^{S-S} and HMGB1^{C45A}. (e) Superimposition of HMGB1^{S-S} and HMGB1^{C106A}.

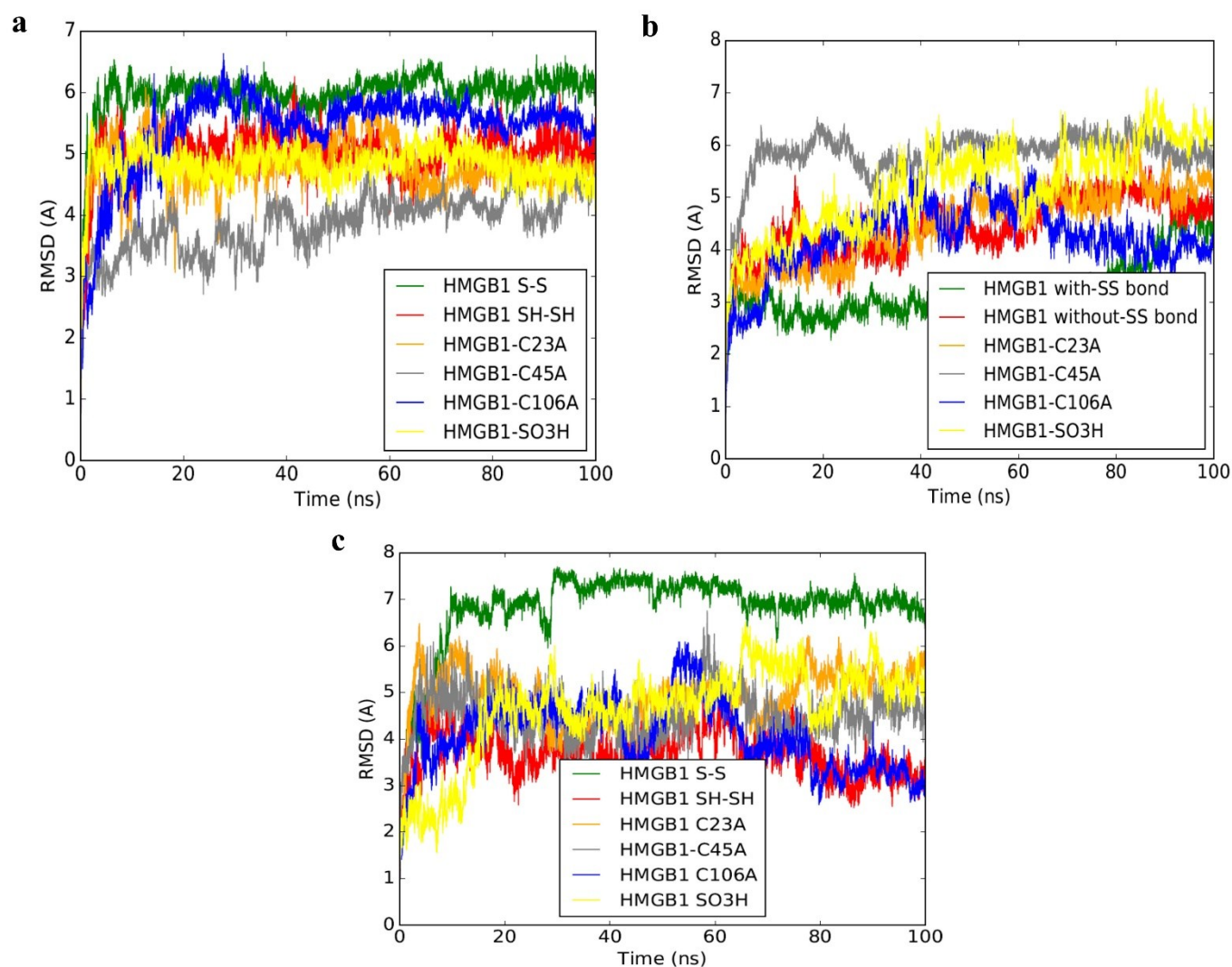


Fig. S10 | Stability of the loops. Color codes: HMGB1^{S-S} (green), HMGB1^{SH-SH} (red), HMGB1^{SO3H} (yellow), HMGB1^{C23A} (orange), and HMGB1^{C106A} (blue). RMSD of (a) Linker loop 1 (residues 80–88). (b) TLR4 binding domain loop (residues 89–108). (c) Linker loop 2 (residues 163–185). Superimposed structures of (d) Linker loop 1. (e) TLR4 binding domain loop and (f) Linker loop 2.

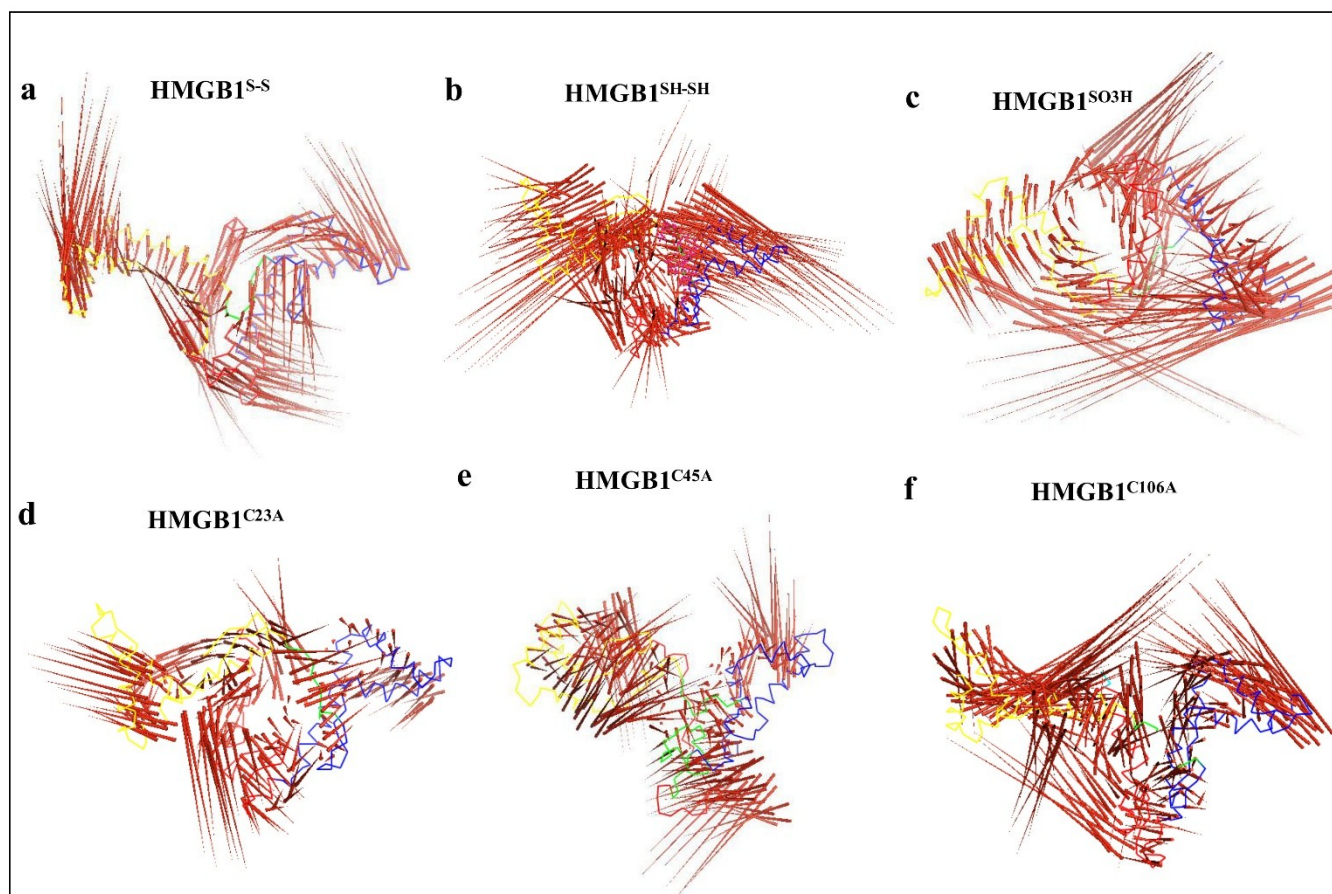


Fig. S11 | Porcupine plots of the first eigenvector. (a) HMGB1^{S-S}; (b) HMGB1^{SH-SH}; (c) HMGB1^{SO3H}; (d) HMGB1^{C23A}, (e) HMGB1^{C45A}, and (f) HMGB1^{C106A}. The A box domain, B box domain, and C-terminal loop are marked in yellow, blue and red, respectively.

Movies S1-S6 | Simulated redox states of HMGB1. The movies show the conformational changes of the domains along the simulation trajectory in the models. The protein is displayed in ribbon representation. Color code: A-box domain (yellow), linker loop1 (green), B-box domain (blue), linker loop2 (pink), TLR4 domain loop (red), and C-terminal tail (orange). The movie was created using PyMOL Molecular Graphics System, Version 1.7.4 Schrödinger, LLC.

Movie S1 | HMGB1^{S-S}

Movie S2 | HMGB1^{SH-SH}

Movie S3 | HMGB1^{SO3H}

Movie S4 | HMGB1^{C23A}

Movie S5 | HMGB1^{C45A}

Movie S6 | HMGB1^{C106A}